ORIGINAL ARTICLE

Microglia of Prefrontal White Matter in Suicide

Tatiana P. Schnieder, PhD, Iskra Trencevska, MPH, Gorazd Rosoklija, MD, PhD, Aleksandr Stankov, MD,
J. John Mann, MD, John Smiley, PhD, and Andrew J. Dwork, MD

Abstract

Immune functions in the brain are associated with psychiatric illness and temporary alteration of mental state. Microglia, the principal brain immunologic cells, respond to changes in the internal brain milieu through a sequence of activated states, each with characteristic function and morphology. To assess a possible association of frontal white matter pathology with suicide, we stained autopsy brain tissue samples from 11 suicide and 25 nonsuicide subjects for ionized calcium-binding adapter molecule 1, cluster of differentiation 68, and myelin. Groups were matched by age, sex, and psychiatric diagnosis. We classified ionized calcium-binding adapter molecule 1–immunoreactive cells based on shape, immunoreactivity to cluster of differentiation 68, and association with blood vessels to obtain stereologic estimates of densities of resting microglia, activated phagocytes, and perivascular cells. We found no effect of psychiatric diagnosis but 2 statistically significant effects of suicide: 1) The dorsal-ventral difference in activated microglial density was reversed such that, with suicide, the density was greater in ventral prefrontal white matter than in dorsal prefrontal white matter, whereas in the absence of suicide, the opposite was true; and 2) with suicide, there was a greater density of ionized calcium-binding adapter molecule 1–immunoreactive cells within or in contact with blood vessel walls in dorsal prefrontal white matter. These observations could reflect a mechanism for the stress/diathesis (state/trait) model of suicide, whereby an acute stress activates a reactive process in the brain, either directly or by compromising the blood-brain barrier, and creates a suicidal state in an individual at risk. They also indicate the theoretical potential of imaging studies in living vulnerable individuals for the assessment of suicide risk. Further studies are needed to investigate specific phenotypes of perivascular cells and blood-brain barrier changes associated with suicide.

Key Words: Blood-brain barrier, Human, Microglia, Perivascular cells, Suicide, White matter.

INTRODUCTION

Every year, approximately 1 million people around the world die by suicide (1). Ninety percent of people who die by suicide in Western countries are diagnosed as having a psychiatric disorder (2), but most mentally ill individuals do not die by suicide, suggesting that factors outside and in addition to the disease may play a role (3, 4).

Evidence pointing to an immunologic component in the etiology of suicide has accumulated in recent years. Distinct in vivo (5–7) and postmortem (8, 9) cytokine profiles distinguish suicide attempters and completers from nonattempters and nonsuicide sudden deaths, respectively. Microglia are the immunologic sentinel cells of the CNS and its main producers of cytokines (10, 11). Changes in microglial morphology and function have been reported in major depression, bipolar disorder, schizophrenia, anxiety disorders, autism spectrum disorders, and suicide (12). Higher microglial cell counts were also detected in the white and gray matter of autopsy brains from psychiatric patients diagnosed as having schizophrenia or affective disorders (13). Radewicz et al (14) found significantly greater densities of microglia in the temporal and frontal cortices from autopsies of individuals with chronic schizophrenia, compared with individuals with no psychiatric diagnosis. A positron emission tomography (PET) study revealed significantly greater levels of mitochondrial translocator protein, which is expressed by activated microglia (and, possibly, by reactive astrocytes) in the gray matter of subjects with recent-onset schizophrenia compared with subjects without psychiatric illness (15, 16). Microglial activation could initiate psychopathology, could be secondary to another process (central or peripheral) that initiates psychopathology, or could be a reaction to psychopathology itself. These possibilities are not mutually exclusive. On the other hand, several studies provide evidence against activation of microglia in psychiatric disease (17–22). Only one of these studies directly investigated microglial activation in brains of suicides and found greater densities of activated microglia in the dorsolateral prefrontal cortex, anterior cingulate cortex, and mediodorsal thalamus in suicides, independent of the psychiatric diagnosis (22).

Immune reactions in the CNS are influenced by its partially privileged and protected environment; it is devoid of lymphatics, contains only small numbers of conventional

antigen-presenting cells, and is isolated by a blood-brain barrier (BBB) that impedes the influx of peripheral immune cells and antibodies (23). However, recent findings speak against the dogma of the brain's stringent impermeability to outside molecules in psychiatric diseases (24) and suicide (25–27). A disruption in the BBB may precede or follow a peripheral or central immune response, leading to an influx of peripheral immune cells, many of which may be found within or in contact with vascular walls. Thus, altered distribution of microglia or peripheral macrophages could be a biomarker of suicidality that might be assessed by in vivo imaging. In addition, these cells may provide a useful target for pharmacologic interventions that deter their harmful effects or enhance their beneficial effects.

Although in vivo studies of suicide attempters and completers point to the vulnerability of white matter (28–31), most autopsy studies of microglia in psychiatric disorders have addressed only gray matter. There have been no prior studies of microglia in white matter in suicide, and there are several reasons to believe that these could be important: a) Microglia are typically much more numerous in white matter than in the corresponding regions of the neocortex (32); b) activation of white matter microglia is a sensitive indicator of subtle damage to white matter, including hypoperfusion associated with aging (33, 34) and normal-appearing white matter in multiple sclerosis (35–40); and c) in vivo imaging with PET can be used to visualize activated microglia. While this method involves exposure to radioactivity and currently is not widely available, diffusion tensor magnetic resonance imaging detects white matter disruption and, if sufficiently sensitive and specific, could be used to predict suicide risk and thus to inform decisions about hospitalization and treatment.

The goal of our study was quantitatively to evaluate microglial cell density in prefrontal white matter. We focused on the prefrontal region because of its role in planning, decision-making, and suppression of impulsiveness (41) (processes that are relevant to suicide) and because numerous studies have found prefrontal differences, largely involving the serotonin system, in autopsy brains of suicides and nonsuicides. Prefrontal cortical abnormalities reported in suicide include lower neuronal density in ventral and dorsal regions (42), less binding of ligands to the serotonin transporter per unit area (43) and per neuron (42) in ventral prefrontal cortex but not in dorsal prefrontal cortex, diminished expression of serotonin 2A receptor in Brodmann area 9 (44), diminished binding of serotonin 1A antagonists in Brodmann area 47 (45), lower levels of messenger RNA for serotonin 2A receptor in dorsolateral prefrontal cortex (44), lower levels of brain-derived neurotrophic factor and its receptor trkB in Brodmann area 9 (46), and increased levels of proinflammatory cytokines in Brodmann area 10 (8).

Because the focus of this study was suicide and not a specific psychiatric illness, the suicide group included individuals with various psychiatric illnesses and without known psychiatric illnesses, and the nonsuicide comparison group included individuals with and without psychiatric disease. We hypothesized that there would be an association between suicide and a higher density of activated phagocytes in prefrontal white matter.

MATERIALS AND METHODS

Human Brain Tissue

Brain tissue was selected from the Macedonian/New York State Psychiatric Institute (NYSPI) brain collection at the Department of Neuropathology and Molecular Imaging, NYSPI. Autopsies were performed at the Institute for Forensic Medicine (Skopje, Macedonia) within 24 hours of death; the median postmortem interval (PMI) for collected specimens was 15 hours. Samples of brain, blood, and urine underwent toxicologic analysis. Structured clinical and demographic evaluations were performed in Macedonia by experienced psychiatrists and psychologists who were trained in these procedures and tested for reliability at the Department of Molecular Imaging and Neuropathology, NYSPI. For all cases, clinical diagnosis was determined by applying *Diagnostic and Statistical Manual of Mental Disorders IV-TR* criteria (47), and the diagnosis was confirmed at a consensus conference attended by senior researchers of the Department of Molecular Imaging and Neuropathology, NYSPI. Diagnostic neuropathologic examination was performed on all fixed hemispheres.

The selection included 11 suicides (mean age, 56 years; 6 women, 5 men) and 25 individuals whose cause of death was not suicide (mean age, 55 years; 12 women, 13 men). Demographic data, clinical diagnoses, and mechanisms of death are presented in Table 1. Among suicide cases, 1 individual with schizoaffective disorder and 1 individual with bipolar disorder were included in the schizophrenia and affective disorders groups, respectively. Two nonsuicides without schizophrenia or affective disorders had a history of alcohol dependence, 1 had an adjustment disorder, 1 had fully remitted bereavement, and 1 had a history of pathologic gambling.

Cases with active infections (<1% of collected cases) or grossly visible lesions in the frontal lobe (mostly gunshot wounds or acute contusions; <5% of collected cases) were excluded in order not to have a handful of cases give rise to skewed distributions of microglial densities. On the other hand, because occult neuropathologic abnormalities are common from the sixth decade onward, other histologic lesions were not excluded so as to avoid bias.

Processing of Tissue

At autopsy, the left hemisphere was sliced in the coronal plane at 2-cm intervals. The slices were placed in homemade cassettes to prevent warping during fixation in approximately 10 vol of phosphate-buffered 10% formalin for 5 days at room temperature. To forestall loss of immunoreactivity associated with prolonged fixation, we stored the slices at 4°C in a large volume of phosphate-buffered saline with 0.02% sodium azide. For this study, a coronal slice of the hemisphere, approximately 4 mm thick, was taken at the level of the rostral tip of the frontal horn of the lateral ventricle (Fig. 1) and subdivided into approximately 8 pieces to fit onto 75 × 25-mm slides. A record was made of the position of each piece. The blocks were embedded in paraffin. Serial 6-μm sections were cut onto charged glass slides (Fisher Super-Frost Plus; Fisher Scientific, Pittsburgh, PA).

TABLE 1. Patient Demographic Data, Psychiatric Diagnoses, and Mechanism of Death

	Suicide (n = 11)	Nonsuicide (n = 25)	Test Statistic	p Value
Age, mean ± SD, years	56 ± 18	55 ± 16	$t_{34} = -0.01$	0.92
Sex	6 F/5 M	12 F/13 M	$\chi^2_1 = 0.1$ (n = 36)	0.72
PMI, mean ± SD, hours	12 ± 8	15 ± 7	$t_{34} = 1.1$	0.28
pH, mean ± SD	6.5 ± 0.2	6.3 ± 0.3	$t_{30} = -0.9$	0.39
Psychiatric diagnosis				
Schizophrenia	2 F/1 M	4 F/3 M	$\chi^2_2 = 5.5$ (n = 36)	0.05
Affective disorders	4 F/1 M	2 F/1 M		
No psychiatric illness	3 M	6 F/9 M		
Mechanism of death, n				
Respiratory	7	4	$\chi^2_4 = 10.5$ (n = 36)	0.03
Traumatic	3	11		
Poisoning	1	1		
Cardiac		7		
Other medical conditions*		2		

*Other medical conditions included iatrogenic thrombocytopenia and hemorrhagic pancreatitis.
F, female; M, male; PMI postmortem interval.

Immunohistochemistry

Two serial sections were processed from each block. To determine microglial phenotype, we performed double bright-field immunostaining on both sections using 2 complementary markers: ionized calcium-binding adapter molecule 1 (Iba-1) and cluster of differentiation 68 (CD68). CD68 (or macrosialin) is a lysosomal membrane marker that is upregulated in phagocytosis (48). Microglia constitutively express CD68 (32). Although ''CD68-immunoreactive microglia'' are often interpreted as activated microglia (49, 50), this presumably refers to microglia recognizable by CD68 staining alone. Iba-1 is a well-established marker for microglia in many mammalian species, including humans (51, 52), and both cell bodies and processes of microglia are strongly immunoreactive to Iba-1. When activated, the cell body enlarges and becomes more strongly immunoreactive to CD68, and the processes become shorter and thicker (53–55). With double labeling, both of these features are apparent, thereby facilitating classification (56, 57). In our material, all Iba-1–immunoreactive cells contained some immunoreactivity to CD68. Iba-1–immunoreactive cells were classified as resting microglia if the processes were thin and CD68 staining occurred predominantly in a punctate distribution (Fig. 2A). (Similar double-labeling patterns were seen in [58] and [59].) Activated microglia had thicker processes and at least 1 focus of CD68 immunoreactivity that was greater than 2.5 μm in diameter (Fig. 2B). Macrophages had rounded cell bodies, few or no processes, and abundant immunoreactivity to CD68 (Fig. 2B).

For statistical analyses, because macrophages accounted for less than 5% of activated phagocytes and because most are probably microglia in advanced stages of activation, counts of activated microglia and macrophages were combined to estimate the density of ''activated phagocytes.'' Because the nature of intravascular and perivascular Iba-1–immunoreactive cells is uncertain, all cells within or in contact with blood vessel walls were classified simply as perivascular. Typically, perivascular cells have ovoid bodies and no visible processes, but the vascular wall often seems to obscure their true shape (Fig. 2C). Counts of activated phagocytes, resting microglia, and perivascular cells were combined to determine total labeled cell density.

After rehydration of paraffin sections and treatment with 3% H_2O_2 (EMD Chemicals Inc, Gibbstown, NJ) for 30 minutes, antigen retrieval was performed by microwaving in Tris/EDTA (Sigma-Aldrich Inc, St Louis, MO) at pH 6.0 until
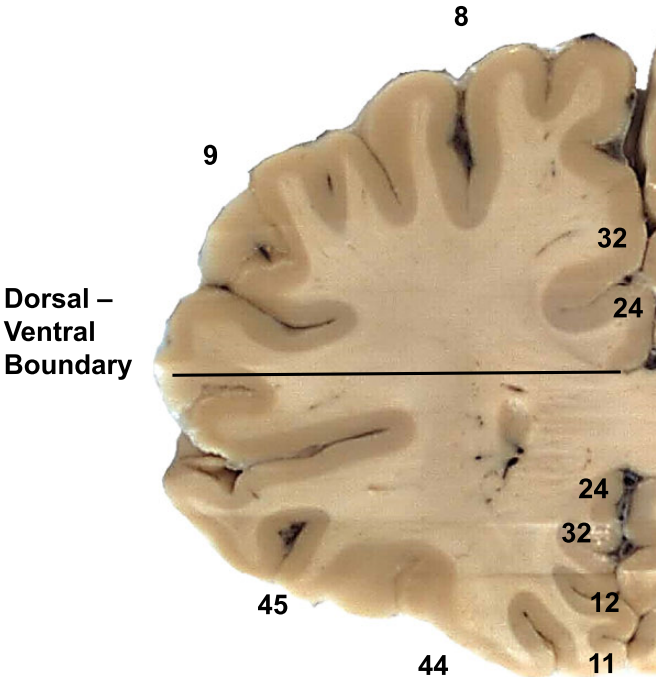

FIGURE 1. Coronal section of the frontal lobe at the level analyzed. As indicated (horizontal line), we subdivided white matter into dorsal and ventral regions at the dorsal edge of the corpus callosum. Sampling was limited to white matter. Brodmann areas are noted for reference.
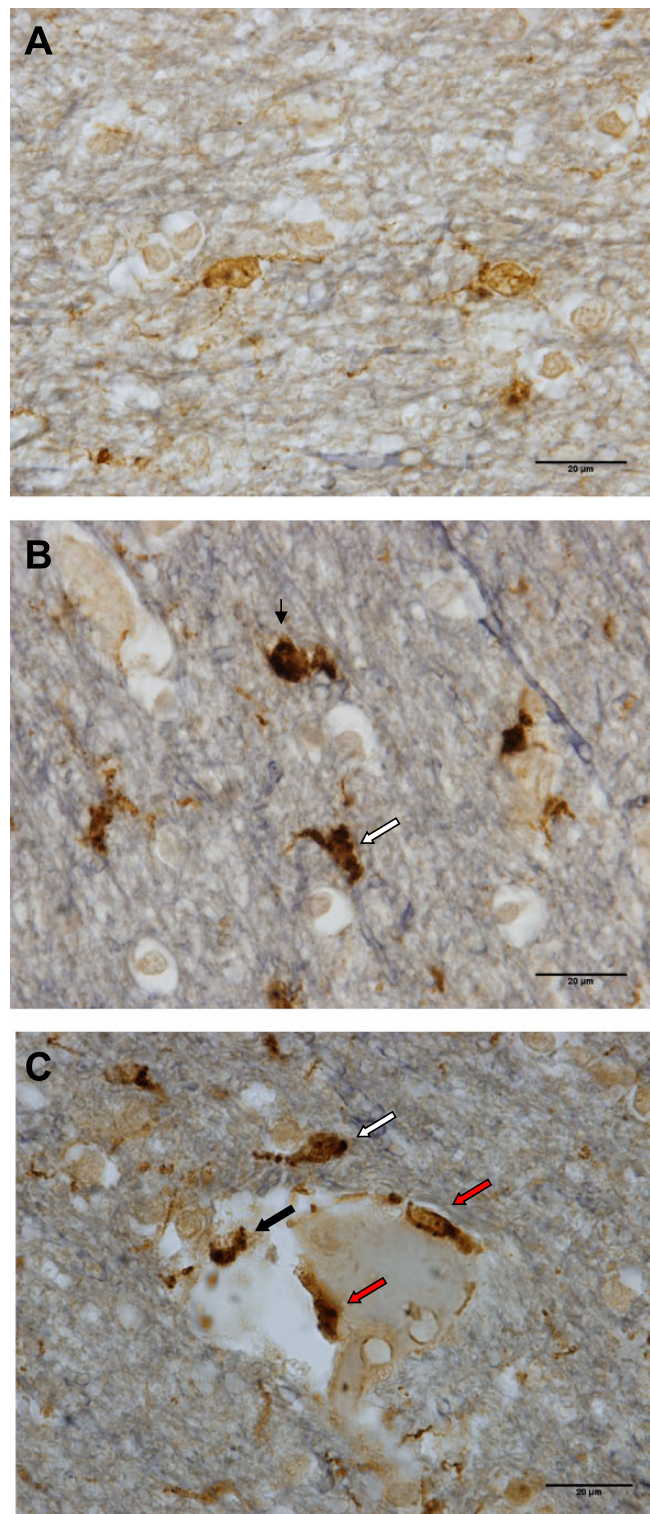
© 2014 American Association of Neuropathologists, Inc.

FIGURE 2. Representative images of microglial phenotypes in human prefrontal white matter, immunostained for Iba-1 (brown) and CD68 (black) with Verhoeff counterstain (gray blue). **(A)** Resting microglia were predominantly Iba-1–immunoreactive with small puncta of immunoreactivity to CD68. **(B)** An activated microglial cell (white arrow) and a macrophage (black arrow) showed strong immunoreactivity to CD68 (black), obscuring much of the Iba-1 staining (brown). **(C)** Immunoreactive cells within (red arrows) or in contact with blood vessel walls (black arrow) were counted as perivascular cells; a cell near the blood vessel, but within the parenchyma (white arrow), was counted as an activated microglial cell. Similar to activated phagocytes, perivascular cells showed strong CD68 immunoreactivity. Scale bar = 20 μm.

boiling for 3 minutes, stopping the microwaving for 5 minutes, replenishing the solution, and microwaving again until boiling for 3 minutes. The sections were then washed with phosphate buffer containing 0.1% Triton X-100 (Fisher Scientific) and covered with 10% normal goat or horse serum (Fisher Scientific) for 1 hour to block nonspecific binding. The slides were placed into individual close-fitting wells in a plastic box (ProHisto LLC, Columbia, SC), in which each was immersed in 2 mL of a 1:500 dilution of anti-CD68 mouse monoclonal IgG (DAKO Corp, Carpinteria, CA) and shaken gently for 3 days. They were then washed, incubated with biotinylated anti-mouse IgG from horse (7.5 µg/mL; whole antibody; Vector Laboratories Inc, Burlingame, CA), washed, incubated with avidin-biotinylated peroxidase complex (Vector Laboratories Inc), washed, and incubated with 0.003% H_2O_2 (EMD Chemicals Inc), 0.02% 3,3'-diaminobenzidine-tetrahydrochloride (Acros Organics, Morris Plains, NJ), and 2% nickel sulfate (Fisher Scientific), yielding a black reaction product. The sections were washed and then incubated with agitation as before overnight at 4°C in a 1:2000 dilution of the second primary antibody, rabbit anti–Iba-1 (Wako Chemicals, Osaka, Japan). Biotinylated secondary antibody and avidin-biotinylated peroxidase complex were applied as before, except without nickel sulfate, so the reaction product was brown.

If the black and brown reaction products appear in exactly the same spot, only the black reaction product is seen because it is darker. As black staining is done first, it does not matter if the peroxidase from that reaction is still active during brown staining because the area is already black and any brown staining will be obscured. On the other hand, because CD68 and Iba-1 are distributed differently within microglial cells, double labeling of cells is easily appreciated. After immunohistochemistry, the sections were lightly counterstained for myelin by the Verhoeff method to provide a clear delineation of white matter (60). Differentiation times were optimized for each staining run to achieve the minimal staining required to produce a visible contrast between gray matter and white matter without compromising immunohistochemical evaluations. Sections were dehydrated and mounted with Permount (Fisher Scientific).

Stereologic Estimation of Microglial Density

All counts were performed, using Visiopharm Software version 3.6.5.0 (Visiopharm, Hørsholm, Denmark), by 1 observer (Tatiana P. Schnieder) who was blind to the identity of the subjects. All counts were conducted with an Olympus BX-61 microscope (Olympus, Center Valley, PA) connected to a motorized 8-slide stage (Prior, Rockland, MA) and a DP71 digital camera (Olympus). A physical disector probe (61) was used to estimate the densities of activated and resting microglia, perivascular cells, and macrophages.

The physical disector method is older and now less familiar than the optical disector (62) but is similar in concept. Both are methods for estimating the number or numeric density of objects in a volume by counting profiles of the objects in slices of the volume. In a randomly placed slice of fixed thickness, the number of profiles will be influenced by the size and orientation of the objects to be counted. Large objects and objects with their longest dimension perpendicular to the plane of section will be more likely to appear than would smaller objects or objects with their longest dimension parallel to the plane of section. This is the commonly referenced problem of ''bias'' (62). A related problem is that, even if one is certain that all of the objects to be counted are identical in size, shape, and orientation, if their length perpendicular to the slice is greater than the thickness of the slice of tissue in which counts are performed, it is not possible to know what that length is; therefore, there is no way to relate the number of profiles to the volume of tissue on the slide. With the optical or physical disector, however, we examine adjacent levels of the tissue to identify and count only the ''first'' appearance of a cell. We only count cells that are identified in a measured deeper portion of the tissue but cannot be identified more superficially. In the case of the optical disector, depth in the tissue is determined by the plane of focus in which the object first appears. One designates a superficial exclusion zone, and only objects that are in focus in the deeper disector zone, but not in the exclusion zone, are counted. The physical disector works identically, but the exclusion zone is 1 of 2 serial sections, and one counts only objects that appear in the other slide, but not in the first. The counting event, with either method, can be the appearance of any aspect of the object that the observer can identify uniquely and consistently, such as the nucleus, nucleolus, or cell body. In our case, the counting event was the first recognizable appearance of the cell body because this was stained intensely and we did not counterstain for nuclei.

There are practical advantages to both the physical disector and the optical disector. The physical disector requires alignment of the slides, which, although performed mostly by the software, must be fine-tuned by the operator. It allows clarity and familiarity of thin paraffin sections and eliminates concerns about penetration of antibodies through thick sections. The physical disector also avoids the optical disector's requirement to determine the exact depth at which an object comes into focus and the reliance of that process on lenses and condensers of high numeric aperture.

To use the physical disector, the software photographed and assembled montages of low-magnification images of the 2 serial 6-µm sections. The edges of white matter from the 2 images were aligned in the software by the operator. The perimeter of white matter was outlined in one of the images (''reference''), and images of uniform random sampling fields were photographed with a 20× dry objective (Olympus UPLFLN; numeric aperture, 0.5), with a 2,000-µm step between each field. Depending on the size of the white matter region, 1 of 3 counting frame sizes was used: 150 × 100, 200 × 150, or 250 × 200 µm². The same fields were photographed in the second (''lookup'') section and carefully aligned by the operator. The counting frame was superimposed on the image by the software. Cells were counted if i) their somas were visible; ii) their somas did not touch the exclusion boundaries of the counting frame; iii) they appeared within the unbiased counting frame applied to the reference section; and iv) they did not appear in the ''lookup'' section (63) (Fig. 3). Except for the corpus callosum, all white matter in the sampled sections was included, regardless of its distance from the cortex.
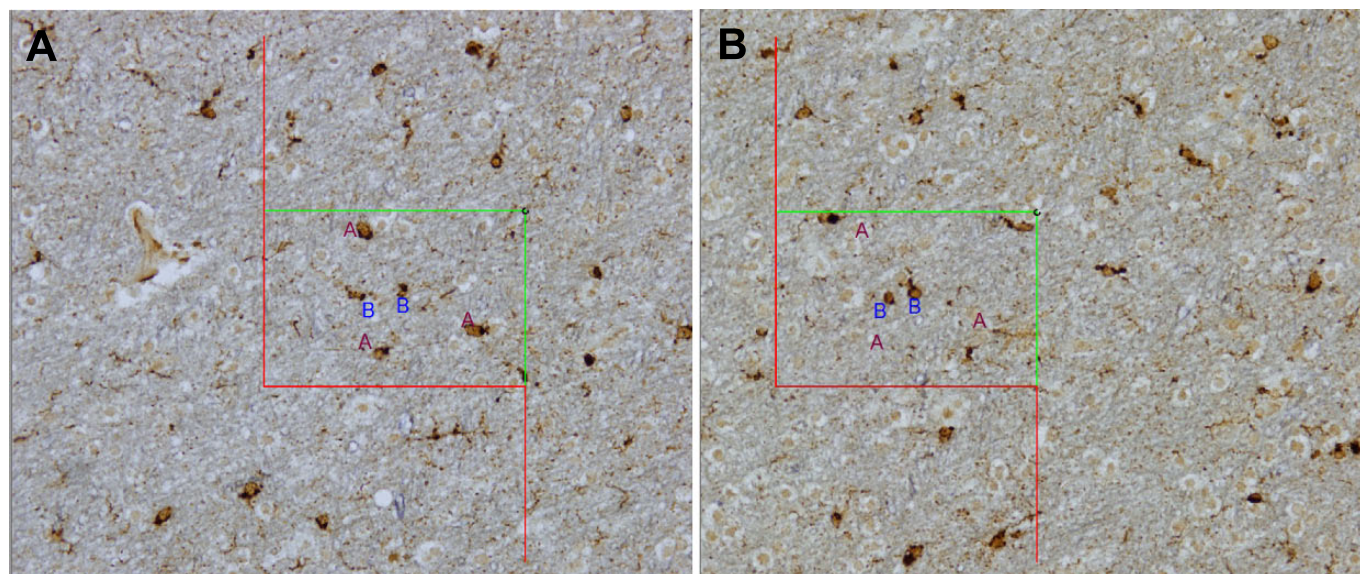
FIGURE 3. Physical disector probe. **(A, B)** After the perimeter of white matter was delineated in a low-magnification photomontage, the magnification was increased 10-fold to acquire "reference" images of uniform random sampling fields, with a 2,000-μm step between each field. The same fields were photographed in the second ("lookup") section and carefully aligned by the operator. The counting frame was superimposed on the image by the software. Cells were counted if i) their somas were visible; ii) they appeared within the unbiased counting frame applied to the "reference" section; iii) their somas did not touch exclusion boundaries; and iv) they did not appear in the "lookup" section (63). Three counted activated microglial cells are marked with the letter "A" within the counting frame in the "reference" section **(A)**, as their cell bodies are clearly visible, they do not touch the red exclusion boundaries, and they do not appear in the "lookup" section **(B)**; 2 microglial cells marked with the letter "B" are not counted because they are also visible in the "lookup" section.

Statistical Analysis

Statistical analyses were performed using SPSS version 21 (SPSS, Chicago, IL). The relationships between age, PMI, brain pH, sex, and cell densities were examined. Because the behavioral functions of dorsal and ventral prefrontal cortex differ (41, 64) and because the ventral cortex is more specifically implicated in suicidality (43, 65–67), we analyzed the 2 regions separately. Thus, there were 6 primary dependent variables: densities of activated phagocytes, resting microglia, and perivascular cells in 2 regions each. In addition, 3 derived variables were assessed as follows: For each cell type, the standardized difference between dorsal and ventral density and the mean of the 2 was computed as

$$\frac{\text{ventral density} - \text{dorsal density}}{\text{ventral density} + \text{dorsal density}}$$

Correlations among the dependent variables and between the dependent variables and age, brain pH, and PMI were determined by linear regression. Suicides and nonsuicides were compared on each dependent variable separately, including age, sex, and PMI as covariates, when significantly correlated with the dependent variable. Because the correlations and comparisons in Table 1 were determined only to inform the comparisons between groups, the significance values for these measures were not adjusted for multiple comparisons. The comparisons of suicides with nonsuicides on each of the 9 dependent variables were evaluated with and without adjustment for multiple comparisons.

On average, 256 counting frames were analyzed and 1,348 cells were counted per subject. Coefficient of error (CE) was estimated to a first approximation for each subject for every cell type in the combined coronal slice and in ventral and dorsal subregions as $CE = 1 / \sqrt{n}$, where n is the number of cells of a particular subtype counted for that subject (68). Values of CE ranged from 0.04 to 0.26 for activated cells, from 0.04 to 0.22 for resting microglia, and from 0.05 to 0.15 for perivascular cells. Coefficient of variation (CV) was computed as $CV = $ standard deviation (SD) / mean density for each cell type in dorsal, ventral, and dorsal-ventral matter for suicide and nonsuicide subjects separately (Table 2). The fractional contribution of estimation error to the variance is given by $(CE / CV)^2$ and ranges from 0.02 to 0.15, indicating that the sampling was adequate; the accuracy of estimates of the means would be much more efficiently improved by increasing the number of subjects than by counting more cells from each subject.

RESULTS

Group Characteristics

There were no differences in pH or PMI between groups separated by sex, manner of death (suicide or nonsuicide), cause of death, or psychiatric diagnosis. Age was different between diagnoses ($F_{2,33} = 4.7$, p = 0.02) because the affective disorders group was older (mean ± SD age, 63.6 ± 11.1 years) than those without psychiatric illness (mean ± SD

TABLE 2. CV and Root Mean Square CE in Dorsal and Ventral White Matter for Suicide and Nonsuicide Deaths

Region	Suicide	Activated Phagocytes			Resting Microglia			Perivascular Cells		
		CV	CE	$\sqrt{CV^2 - CE^2}$	CV	CE	$\sqrt{CV^2 - CE^2}$	CV	CE	$\sqrt{CV^2 - CE^2}$
Dorsal	No	0.42	0.07	0.41	0.45	0.08	0.44	0.23	0.08	0.22
Dorsal	Yes	0.46	0.07	0.45	0.36	0.07	0.35	0.19	0.07	0.18
Ventral	No	0.52	0.10	0.51	0.36	0.09	0.35	0.27	0.09	0.25
Ventral	Yes	0.34	0.07	0.33	0.34	0.07	0.33	0.23	0.08	0.22

The normalized variance for each measure within each group (suicide and nonsuicide), CV^2, contains a contribution, CE^2, from the error introduced into each measurement by counting systematic random samples rather than counting all of the cells of a given type, plus a contribution, $CV^2 - CE^2$, from the true variation among cases in the group. Thus, the minimal CV that can be obtained by counting more cells per subject is $\sqrt{CV^2 - CE^2}$. Any further reduction in the uncertainty of the mean (normalized standard error = $CV/\sqrt{N-1}$) can be achieved only by increasing N, which is the number of subjects in the group.

CV, group SD/group mean; CE, root mean square of theoretical CE for each case in the group.

age, 47.7 ± 17.3 years). Men (mean ± SD age, 49.2 ± 18.1 years) were younger than women (mean ± SD age, 61.1 ± 11.8 years) ($t = 2.3$, $df = 344$, $p = 0.03$). In addition, pH was inversely related to age ($r = -0.42$, $p = 0.02$). There were no effects of prescribed psychotropic medications or any significant interaction effects between manner of death and psychiatric diagnosis on any of the dependent variables. All tests were 2-tailed.

Significant Correlations

Correlations among the 6 primary dependent variables and between them and age, brain pH, and PMI are listed in Table 3. The 3 measures derived from dorsoventral comparisons were not correlated with each other or with age, sex, or PMI, so the 3 comparisons were performed without covariates. At the level of individual slides, resting microglia were negatively correlated with activated phagocytes ($r = -0.53$, $p < 0.0005$); neither correlated significantly with perivascular cells ($-0.1 < r < 0.1$).

Differences Between Suicides and Nonsuicides

All density measurements are listed in Table 4. There were no significant effects of suicide on densities of resting or activated microglia in dorsal or ventral prefrontal white matter, but the density of perivascular cells in dorsal white matter was 18% higher in suicides than in nonsuicides ($t = 2.2$, $df = 34$, unadjusted $p = 0.033$). In ventral white matter, there was no significant difference between suicides and nonsuicides (unadjusted $p > 0.5$). Normalized dorsal-ventral differences for resting and perivascular cells were positive for both suicides and nonsuicides and approximately 30% greater in suicides than in nonsuicides; the differences were not statistically significant ($p > 0.4$). Densities of activated phagocytes were greater ventrally than dorsally among suicides, however, and greater dorsally than ventrally among nonsuicides (Fig. 4; $t = 3.4$, $df = 34$, unadjusted $p = 0.0015$).

If one corrects conservatively for multiple comparisons, the association of suicide with an altered dorsal-ventral gradient in the density of activated phagocytes remains significant. On Holm-Bonferroni correction (69), for the most significant of 9 members in a family of tests, the stated significance level is divided by 9. Thus, for an α of 0.05, the criterion becomes $p < 0.0056$, which is met. Once the first null hypothesis is rejected, the criterion for the second most significant result (higher perivascular cell density in dorsal white matter of suicide cases than of nonsuicide cases) becomes $\alpha / 8$ or $p < 0.0063$, which is not met by $p = 0.033$. The probability of type 1 error for at least 1 of 8 independent tests at $p = 0.033$ is $1 - (1 - 0.033)^8 = 0.24$. However, the tests are not independent; in fact, both the increased number of dorsal perivascular cells and the increased ratio of ventral to dorsal activated cell density could result from a preferential localization of activated phagocytes in dorsal prefrontal white matter to blood vessels and perivascular space in suicidal

TABLE 3. Correlation Coefficients Among Primary Variables

	Activated Phagocytes, Dorsal	Activated Phagocytes, Ventral	Resting Microglia, Dorsal	Resting Microglia, Ventral	Perivascular Cells, Dorsal	Perivascular Cells, Ventral	PMI	pH
Activated phagocytes, ventral	0.787*							
Resting microglia, dorsal	−0.596*	−0.444*						
Resting microglia, ventral	−0.449*	−0.463*	0.738*					
Perivascular cells, dorsal	−0.006	−0.035	−0.040	0.084				
Perivascular cells, ventral	0.147	0.238	−0.140	−0.111	0.368†			
PMI	−0.015	−0.171	−0.237	−0.113	0.034	0.461*		
pH	−0.188	0.033	0.450*	0.314	0.108	0.068	−0.131	
Age	0.029	0.053	−0.110	−0.012	0.057	0.204	−0.112	−0.421†

Correlation coefficients are expressed as *r* values.
*Correlation is significant at the 0.01 level (2-tailed).
†Correlation is significant at the 0.05 level (2-tailed).

TABLE 4. Cell Densities, by Manner of Death, in Dorsal and Ventral Prefrontal White Matter

	Suicide (n = 11)		Nonsuicide (n = 25)	
	Dorsal	**Ventral**	**Dorsal**	**Ventral**
Activated phagocytes	5,592 ± 2,578	6,620 ± 2,247	6,901 ± 2,887	6,039 ± 3,120
Resting microglia	6,292 ± 2,267	7,001 ± 2,415	5,868 ± 2,666	6,897 ± 2,489
Perivascular cells	4,684* ± 884	4,808 ± 1,104	3,967 ± 893	4,531 ± 1,214
Total labeled cells	16,567 ± 1,666	18,431 ± 3,234	16,736 ± 2,888	17,467 ± 3,152

Data are expressed in cells per cubic millimeter and presented as mean ± SD.
*$p < 0.05$ (significantly different from nonsuicides).

individuals. It should be noted also that the effect size was 0.8, yielding a power of 0.6 to detect an effect at an α of 0.05 but only a power of 0.3 at an α of 0.0063.

DISCUSSION

We found no effect of psychiatric diagnosis, but there were significant effects of suicide on density of activated phagocytes in ventral prefrontal white matter relative to dorsal prefrontal white matter and possibly on density of microglia-like cells within or in contact with blood vessel walls in dorsal prefrontal white matter. This was a small study that must be replicated. The first finding remains statistically significant after adjusting for multiple statistical tests, but the second finding does not. However, the second result is plausible and consistent with the first result.

In all areas analyzed, densities of activated cells correlated positively with total cell density (data not shown) and negatively with resting cell density, suggesting that activating stimuli promote both conversion from resting state to active state and recruitment or proliferation.

Potential Role of Microglia in Suicide

Suicide is often viewed as a combination of 2 components: a long-standing trait or diathesis of susceptibility and an acute stress or trigger. Autoimmunity can have a parallel structure. For example, in a mouse model of systemic lupus erythematous, there is a state of production of antibodies to double-stranded DNA; this state does not affect the brain until stress compromises the BBB. This allows the entry of the antibodies, which cross-react with subunits of the *N*-methyl-D-aspartate receptor, enhancing its activation by glutamate. The enhanced activation produces behavioral changes and—if the compromise of the BBB persists—destruction of brain tissue (70, 71). Stress can also allow recruitment of splenic or bone marrow monocytes to the brain and their accumulation in perivascular spaces, resulting in anxiety-like behaviors that can be prevented if the supply of peripheral monocytes is depleted (e.g. by splenectomy) (72, 73).

The possibility of an autoimmune basis for some cases of suicide is supported by the finding that antibodies to serotonin were present in more than half of cases of major depression (compared with fewer than 10% of individuals without depression) and were found in all cases of depression with elevated proinflammatory cytokines (74). Presumably, an autoimmune process directed against serotonin could remove serotonergic axons or their terminals and account for deficits in serotonin, its transporter, and its presynaptic receptors. This

speculation is also consistent with the dorsal-ventral specificity of our findings because the transporter deficiency associated with suicide is predominantly ventral (43).

Low serotonin transporter binding could be caused by reduced intrasynaptic serotonin (75). It is possible that serotonin levels are depleted by activated microglia that have enhanced metabolism of tryptophan to quinolinic acid via the kynurenine pathway (76). Cytokines are known to enhance the kynurenine pathway in microglia, and quinolinic acid can activate *N*-methyl-D-aspartate receptors and possibly disrupt the BBB (77). As a result, quinolinic acid could increase stimulation of neurons in ventral prefrontal cortex and lead to a loss of normal connectivity with the limbic system and impaired impulse control. Because our study was confined to white matter, correlations with cortical abnormalities are speculative.

Potential Clinical Importance

A potentially important implication of the different dorsoventral distribution of activated phagocytes in suicide is that it could be detected in in vivo PET with ligands for the mitochondrial translocator protein (formerly the peripheral benzodiazepine receptor) (30). These receptors are expressed by reactive microglia and possibly astrocytes (78). Although
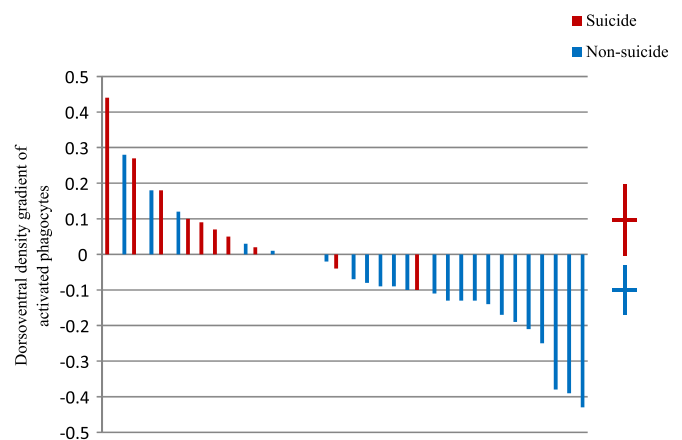

FIGURE 4. Significant association of suicide with distribution of activated phagocytes. Dorsoventral gradient of activated cell density, computed as (ventral density − dorsal density) / (ventral density + dorsal density). Suicide (red) was associated with a ventral > dorsal gradient, whereas nonsuicide death (blue) was associated with a dorsal > ventral gradient ($t_{34} = 3.4$, $p = 0.002$). Means and 95% confidence intervals for each group's gradient are shown on the right.

the affinity of the most specific radioligand currently available is also influenced by a genetic polymorphism (79), this can be determined by genotyping. In any event, genetic and other factors that globally influence PET signal would affect dorsal and ventral prefrontal cortex binding comparably, without obscuring a dorsal-ventral difference. Similarly, the dorsal-ventral comparison in our study should not be influenced by shrinkage, extent of fixation, PMI, or other confounds that could globally influence measurements of cellular density. With regard to the implications of our findings for measurable biomarkers of suicide, it should also be noted that methods are undergoing development to track the influx of peripheral phagocytes to the CNS by transport of radioactive or para-magnetic tracers (80). Less specifically, the microglial changes might be associated with changes in diffusion of water in white matter, which could in theory be detected by diffusion tensor imaging.

Implications of Perivascular Cells

Between-subjects analyses failed to reveal any significant difference in the densities of resting or activated cells between suicide and nonsuicide subjects. Moreover, contrary to our prediction, in suicides, there was a trend toward a lower density of activated cells in dorsal white matter. However, in the same region, suicide was associated with an 18% greater density of perivascular cells. Although we do not yet know their source, the finding of perivascular accumulations of phagocytes in suicide strengthens the idea of changes in the properties of the BBB. If both peripheral and CNS immune cells increase cytokine secretion and increase exchange across the BBB, a feed-forward inflammatory prelude to suicide could result (81).

At first glance, our findings of increased density of perivascular cells, but not of activated phagocytes, in dorsal white matter contrast with the findings of increased density of activated microglia in dorsolateral frontal white matter in suicide (22). However, Steiner et al (22) classified perivascular human leukocyte antigen D-related (HLA-DR) -immunoreactive cells as amoeboid reactive microglia, whereas we chose to place perivascular cells in a separate category because their nature is uncertain. These cells could be juxtavascular microglia (82, 83), perivascular macrophages (84–86), or pericytes (87, 88), or some mixture of these.

Limitations

Our study includes certain limitations. The sample size was small, and only white matter was analyzed. The main drawback of any postmortem brain study is the inability to draw causal conclusions from correlational data at a single—albeit in this case critical—point in time. Another concern relates to the evaluation of microglial activation. Microglia with a classical ''resting'' morphology perform sentinel and reparative functions in the brain. Nonetheless, there is little doubt that the microglia that we classified as activated, with short and thick or absent processes and increased immunoreactivity to CD68, represent phagocytically active cells.

Another limitation is that we did not use a specific stain for blood vessels and hence may have underestimated the density of perivascular cells. However, such a bias would presumably be independent of suicide. Finally, although we used a physical disector probe to obtain unbiased cell density measurements within the processed tissue, we cannot know how much these were affected by shrinkage of tissue during fixation and processing for paraffin embedding. Although this means that the absolute densities that we have obtained may be different from those obtained with tissue processed differently, we obtain essentially identical levels of statistical significance, or lack thereof, if we eliminate effects of shrinkage by analyzing densities of individual cell types as a fraction of the total density of Iba-1–immunoreactive cells.

In conclusion, this study, though small and requiring replication, provides evidence for the presence of abnormal densities of phagocytic cells in prefrontal white matter in individuals who committed suicide. These may prove useful for future prediction and prevention of suicide.

REFERENCES

1. World Health Organizaton. The World Health Report Chapter 1. Available at: http://www.who.int/whr/2003/en/Chapter1-en.pdf2003.2014 Accessed February 14, 2014
2. Bertolote JM, Fleischmann A. Suicide and psychiatric diagnosis: A worldwide perspective. World Psychiatry 2002;1:181–85
3. Brent DA, Oquendo M, Birmaher B, et al. Familial pathways to early-onset suicide attempt: Risk for suicidal behavior in offspring of mood-disordered suicide attempters. Arch Gen Psychiatry 2002;59:801–7
4. Baldessarini RJ, Hennen J. Genetics of suicide: An overview. Harv Rev Psychiatry 2004;12:1–13
5. Janelidze S, Mattei D, Westrin A, et al. Cytokine levels in the blood may distinguish suicide attempters from depressed patients. Brain Behav Immun 2011;25:335–39
6. Lindqvist D, Janelidze S, Hagell P, et al. Interleukin-6 is elevated in the cerebrospinal fluid of suicide attempters and related to symptom severity. Biol Psychiatry 2009;66:287–92
7. Lindqvist D, Janelidze S, Erhardt S, et al. CSF biomarkers in suicide attempters—a principal component analysis. Acta Psychiatr Scand 2011; 124:52–61
8. Pandey GN, Rizavi HS, Ren X, et al. Proinflammatory cytokines in the prefrontal cortex of teenage suicide victims. J Psychiatr Res 2012; 46:57–63
9. Tonelli LH, Stiller J, Rujescu D, et al. Elevated cytokine expression in the orbitofrontal cortex of victims of suicide. Acta Psychiatr Scand 2008; 117:198–206
10. Frank MG, Baratta MV, Sprunger DB, et al. Microglia serve as a neuro-immune substrate for stress-induced potentiation of CNS pro-inflammatory cytokine responses. Brain Behav Immun 2007;21:47–59
11. Hanisch UK. Microglia as a source and target of cytokines. Glia 2002; 40:140–55
12. Frick LR, Williams K, Pittenger C. Microglial dysregulation in psychiatric disease. Clin Dev Immunol 2013;2013:608654
13. Bayer TA, Buslei R, Havas L, et al. Evidence for activation of microglia in patients with psychiatric illnesses. Neurosci Lett 1999;271:126–28
14. Radewicz K, Garey LJ, Gentleman SM, et al. Increase in HLA-DR immunoreactive microglia in frontal and temporal cortex of chronic schizophrenics. J Neuropathol Exp Neurol 2000;59:137–50
15. van Berckel BN, Bossong MG, Boellaard R, et al. Microglia activation in recent-onset schizophrenia: A quantitative (*R*)-[¹¹C]PK11195 positron emission tomography study. Biol Psychiatry 2008;64:820–22
16. Doorduin J, de Vries EF, Willemsen AT, et al. Neuroinflammation in schizophrenia-related psychosis: A PET study. J Nucl Med 2009;50: 1801–7
17. Arnold SE, Trojanowski JQ, Gur RE, et al. Absence of neuro-degeneration and neural injury in the cerebral cortex in a sample of elderly patients with schizophrenia. Arch Gen Psychiatry 1998;55: 225–32

© 2014 American Association of Neuropathologists, Inc.

18. Falke E, Han LY, Arnold SE. Absence of neurodegeneration in the thalamus and caudate of elderly patients with schizophrenia. Psychiatry Res 2000;93:103–10

19. Kurumaji A, Wakai T, Toru M. Decreases in peripheral-type benzodiazepine receptors in postmortem brains of chronic schizophrenics. J Neural Transm 1997;104:1361–70

20. Togo T, Akiyama H, Kondo H, et al. Expression of CD40 in the brain of Alzheimer's disease and other neurological diseases. Brain Res 2000; 885:117–21

21. Schnieder TP, Dwork AJ. Searching for neuropathology: Gliosis in schizophrenia. Biol Psychiatry 2011;69:134–39

22. Steiner J, Bielau H, Brisch R, et al. Immunological aspects in the neurobiology of suicide: Elevated microglial density in schizophrenia and depression is associated with suicide. J Psychiatr Res 2008;42:151–57

23. Zlokovic BV. The blood-brain barrier in health and chronic neurodegenerative disorders. Neuron 2008;57:178–201

24. Shalev H, Serlin Y, Friedman A. Breaching the blood-brain barrier as a gate to psychiatric disorder. Cardiovasc Psychiatry Neurol 2009;2009: 278531

25. Falcone T, Fazio V, Lee C, et al. Serum S100B: A potential biomarker for suicidality in adolescents? PLoS One 2010;5:e11089

26. Miguel-Hidalgo JJ, Overholser JC, Jurjus GJ, et al. Vascular and extravascular immunoreactivity for intercellular adhesion molecule 1 in the orbitofrontal cortex of subjects with major depression: Age-dependent changes. J Affect Disord 2011;132:422–31

27. Bayard-Burfield L, Alling C, Blennow K, et al. Impairment of the blood-CSF barrier in suicide attempters. Eur Neuropsychopharmacol 1996;6:195–99

28. Olvet DM, Peruzzo D, Thapa-Chhetry B, et al. A diffusion tensor imaging study of suicide attempters. J Psychiatr Res 2014;51:60–67

29. Desmyter S, van Heeringen C, Audenaert K. Structural and functional neuroimaging studies of the suicidal brain. Prog Neuropsychopharmacol Biol Psychiatry 2011;35:796–808

30. Jollant F, Lawrence NL, Olie E, et al. The suicidal mind and brain: A review of neuropsychological and neuroimaging studies. World J Biol Psychiatry 2011;12:319–39

31. Pompili M, Serafini G, Innamorati M, et al. White matter hyperintensities, suicide risk and late-onset affective disorders: An overview of the current literature. Clin Ter 2010;161:555–63

32. Mittelbronn M, Dietz K, Schluesener HJ, et al. Local distribution of microglia in the normal adult human central nervous system differs by up to one order of magnitude. Acta Neuropathol 2001;101:249–55

33. Fernando MS, Simpson JE, Matthews F, et al. White matter lesions in an unselected cohort of the elderly: Molecular pathology suggests origin from chronic hypoperfusion injury. Stroke 2006;37:1391–98

34. Black S, Gao F, Bilbao J. Understanding white matter disease: Imaging-pathological correlations in vascular cognitive impairment. Stroke 2009; 40:S48–52

35. Allen IV, McQuaid S, Mirakhur M, et al. Pathological abnormalities in the normal-appearing white matter in multiple sclerosis. Neurol Sci 2001; 22:141–44

36. Zeis T, Graumann U, Reynolds R, et al. Normal-appearing white matter in multiple sclerosis is in a subtle balance between inflammation and neuroprotection. Brain 2008;131:288–303

37. Moll NM, Rietsch AM, Thomas S, et al. Multiple sclerosis normal-appearing white matter: Pathology-imaging correlations. Ann Neurol 2011;70:764–73

38. Markoullis K, Sargiannidou I, Schiza N, et al. Gap junction pathology in multiple sclerosis lesions and normal-appearing white matter. Acta Neuropathol 2012;123:873–86

39. van Horssen J, Singh S, van der Pol S, et al. Clusters of activated microglia in normal-appearing white matter show signs of innate immune activation. J Neuroinflamm 2012;9:156

40. Melief J, Schuurman KG, van de Garde MD, et al. Microglia in normal appearing white matter of multiple sclerosis are alerted but immuno-suppressed. Glia 2013;61:1848–61

41. Miller EK, Cohen JD. An integrative theory of prefrontal cortex function. Annu Rev Neurosci 2001;24:167–202

42. Underwood MD, Kassir SA, Bakalian MJ, et al. Neuron density and serotonin receptor binding in prefrontal cortex in suicide. Int J Neuropsychopharmacol 2012;15:435–47

43. Mann JJ, Huang YY, Underwood MD, et al. A serotonin transporter gene promoter polymorphism (5-HTTLPR) and prefrontal cortical binding in major depression and suicide. Arch Gen Psychiatry 2000;57:729–38

44. Sequeira A, Morgan L, Walsh DM, et al. Gene expression changes in the prefrontal cortex, anterior cingulate cortex and nucleus accumbens of mood disorders subjects that committed suicide. PLoS One 2012;7: e35367

45. Stockmeier CA, Howley E, Shi X, et al. Antagonist but not agonist labeling of serotonin-1A receptors is decreased in major depressive disorder. J Psychiatr Res 2009;43:887–94

46. Dwivedi Y, Rizavi HS, Conley RR, et al. Altered gene expression of brain-derived neurotrophic factor and receptor tyrosine kinase B in postmortem brain of suicide subjects. Arch Gen Psychiatry 2003;60: 804–15

47. American Psychiatric Association Task Force on DSM-IV. *Diagnostic and Statistical Manual of Mental Disorders: DSM-IV-TR*. 4th ed. Washington, DC: American Psychiatric Association; 2000:943

48. Rezaie P, Dean A, Male D, et al. Microglia in the cerebral wall of the human telencephalon at second trimester. Cereb Cortex 2005;15:938–49

49. Chung ES, Chung YC, Bok E, et al. Fluoxetine prevents LPS-induced degeneration of nigral dopaminergic neurons by inhibiting microglia-mediated oxidative stress. Brain Res 2010;1363:143–50

50. Chung YC, Kim SR, Jin BK. Paroxetine prevents loss of nigrostriatal dopaminergic neurons by inhibiting brain inflammation and oxidative stress in an experimental model of Parkinson's disease. J Immunol 2010; 185:1230–37

51. Ito D, Tanaka K, Suzuki S, et al. Enhanced expression of Iba1, ionized calcium-binding adapter molecule 1, after transient focal cerebral ischemia in rat brain. Stroke 2001;32:1208–15

52. Hirayama A, Okoshi Y, Hachiya Y, et al. Early immunohistochemical detection of axonal damage and glial activation in extremely immature brains with periventricular leukomalacia. Clin Neuropathol 2001;20:87–91

53. Supramaniam V, Vontell R, Srinivasan L, et al. Microglia activation in the extremely preterm human brain. Pediatr Res 2013;73:301–9

54. Zotova E, Bharambe V, Cheaveau M, et al. Inflammatory components in human Alzheimer's disease and after active amyloid-beta42 immunization. Brain 2013;136:2677–96

55. de Hoz R, Gallego BI, Ramirez AI, et al. Rod-like microglia are restricted to eyes with laser-induced ocular hypertension but absent from the microglial changes in the contralateral untreated eye. PLoS One 2013;8: e83733

56. Loane DJ, Kumar A, Stoica BA, et al. Progressive neurodegeneration after experimental brain trauma: Association with chronic microglial activation. J Neuropathol Exp Neurol 2014;73:14–29

57. Cherry JD, Liu B, Frost JL, et al. Galactic cosmic radiation leads to cognitive impairment and increased abeta plaque accumulation in a mouse model of Alzheimer's disease. PLoS One 2012;7:e53275

58. Michalski D, Heindl M, Kacza J, et al. Spatio-temporal course of macrophage-like cell accumulation after experimental embolic stroke depending on treatment with tissue plasminogen activator and its combination with hyperbaric oxygenation. Eur J Histochem 2012;56:e14

59. Jeong HK, Ji KM, Kim J, et al. Repair of astrocytes, blood vessels, and myelin in the injured brain: Possible roles of blood monocytes. Mol Brain 2013;6:28

60. Sheaffer S, Rosoklija G, Dwork AJ. Myelin staining of archival brain tissue. Clin Neuropathol 1999;18:313–17

61. Braendgaard H, Gundersen HJ. The impact of recent stereological advances on quantitative studies of the nervous system. J Neurosci Methods 1986;18:39–78

62. West MJ, Gundersen HJ. Unbiased stereological estimation of the number of neurons in the human hippocampus. J Comp Neurol 1990;296:1–22

63. Gundersen HJ. Stereology of arbitrary particles. A review of unbiased number and size estimators and the presentation of some new ones, in memory of William R. Thompson. J Microsc 1986;143:3–45

64. Koenigs M, Grafman J. The functional neuroanatomy of depression: Distinct roles for ventromedial and dorsolateral prefrontal cortex. Behav Brain Res 2009;201:239–43

65. Oquendo MA, Placidi GP, Malone KM, et al. Positron emission tomography of regional brain metabolic responses to a serotonergic challenge and lethality of suicide attempts in major depression. Arch Gen Psychiatry 2003;60:14–22

66. Amen DG, Prunella JR, Fallon JH, et al. A comparative analysis of completed suicide using high resolution brain SPECT imaging. J Neuropsychiatry Clin Neurosci 2009;21:430–39
67. Jollant F, Bellivier F, Leboyer M, et al. Impaired decision making in suicide attempters. Am J Psychiatry 2005;162:304–10
68. Bailey T, Gatrell A. *Interactive Spatial Data Analysis*. 1st ed. New York, NY: Wiley and Sons; 1995
69. Holm S. A simple sequentially rejective multiple test procedure. Scand J Stat 1979;6:65–70
70. Diamond B, Volpe BT. A model for lupus brain disease. Immunol Rev 2012;248:56–67
71. Faust TW, Chang EH, Kowal C, et al. Neurotoxic lupus autoantibodies alter brain function through two distinct mechanisms. Proc Natl Acad Sci U S A 2010;107:18569–74
72. Wohleb ES, Powell ND, Godbout JP, et al. Stress-induced recruitment of bone marrow–derived monocytes to the brain promotes anxiety-like behavior. J Neurosci 2013;33:13820–33
73. Wohleb ES, McKim DB, Shea DT, et al. Re-establishment of anxiety in stress-sensitized mice is caused by monocyte trafficking from the spleen to the brain. Biol Psychiatry 2014;75:970–81
74. Maes M, Ringel K, Kubera M, et al. Increased autoimmune activity against 5-HT: A key component of depression that is associated with inflammation and activation of cell-mediated immunity, and with severity and staging of depression. J Affect Disord 2012;136:386–92
75. Chung YC, Kim SR, Park JY, et al. Fluoxetine prevents MPTP-induced loss of dopaminergic neurons by inhibiting microglial activation. Neuropharmacology 2011;60:963–74
76. Steiner J, Walter M, Gos T, et al. Severe depression is associated with increased microglial quinolinic acid in subregions of the anterior cingulate gyrus: Evidence for an immune-modulated glutamatergic neurotransmission? J Neuroinflamm 2011;8:94
77. Guillemin GJ. Quinolinic acid, the inescapable neurotoxin. FEBS J 2012;279:1356–65
78. Cosenza-Nashat M, Zhao ML, Suh HS, et al. Expression of the translocator protein of 18 kDa by microglia, macrophages and astrocytes based on immunohistochemical localization in abnormal human brain. Neuropathol Appl Neurobiol 2009;35:306–28
79. Owen DR, Yeo AJ, Gunn RN, et al. An 18-kDa translocator protein (TSPO) polymorphism explains differences in binding affinity of the PET radioligand PBR28. J Cereb Blood Flow Metab 2012;32:1–5
80. Stoll G, Bendszus M. New approaches to neuroimaging of central nervous system inflammation. Curr Opin Neurol 2010;23:282–86
81. Konsman JP, Drukarch B, Van Dam AM. (Peri)vascular production and action of pro-inflammatory cytokines in brain pathology. Clin Sci (Lond) 2007;112:1–25
82. Graeber MB, Streit WJ, Kreutzberg GW. Identity of ED2-positive perivascular cells in rat brain. J Neurosci Res 1989;22:103–6
83. Grossmann R, Stence N, Carr J, et al. Juxtavascular microglia migrate along brain microvessels following activation during early postnatal development. Glia 2002;37:229–40
84. Fabriek BO, Van Haastert ES, Galea I, et al. CD163-positive perivascular macrophages in the human CNS express molecules for antigen recognition and presentation. Glia 2005;51:297–305
85. Kim WK, Alvarez X, Fisher J, et al. CD163 identifies perivascular macrophages in normal and viral encephalitic brains and potential precursors to perivascular macrophages in blood. Am J Pathol 2006;168:822–34
86. Mato M, Ookawara S, Sakamoto A, et al. Involvement of specific macrophage-lineage cells surrounding arterioles in barrier and scavenger function in brain cortex. Proc Natl Acad Sci U S A 1996;93:3269–74
87. Thomas WE. Brain macrophages: On the role of pericytes and perivascular cells. Brain Res Brain Res Rev 1999;31:42–57
88. Dore-Duffy P, Cleary K. Morphology and properties of pericytes. Methods Mol Biol 2011;686:49–68